

## Effect of High-Energy Ball Milling on the Structure and Mechanical Properties of Ultra-High Molecular Weight Polyethylene

A. V. Maksimkin, S. D. Kaloshkin, V. V. Tcherdyntsev, D. I. Chukov, I. V. Shchetinin

National University of Science and Technology "MISIS", Moscow 119049, Russia

Correspondence to: A. V. Maksimkin (E-mail: aleksey\_maksimkin@mail.ru)

**ABSTRACT:** The structure and properties of ultrahigh-molecular-weight polyethylene (UHMWPE) powder after severe deformation processing in a planetary ball mill were studied by means of scanning electron microscopy, differential scanning calorimetry, and X-ray analysis. We found that the severe deformation processing of UHMWPE changed the morphology of the powder and caused amorphization and partial changes in the structure of the crystalline phase. Monolithic samples were obtained from the pretreated polymer with a hot-pressing method in a wide range of temperatures. The effect of preliminary deformation processing on the mechanical properties of UHMWPE was studied. It was revealed that during monolitization in its melting temperature range, the mechanical properties of the powder increased, whereas the percentage elongation decreased. © 2013 Wiley Periodicals, Inc. *J. Appl. Polym. Sci.* 000: 000–000, 2013

**KEYWORDS:** differential scanning calorimetry (DSC); mechanical properties; morphology; structure–property relations

Received 10 January 2013; accepted 22 April 2013; Published online

DOI: 10.1002/app.39457

### INTRODUCTION

The unique combination of physical and mechanical properties, high wear resistance, low friction coefficient, high chemical resistance, and biocompatibility to living tissues has attracted much attention to ultra-high molecular weight polyethylene (UHMWPE) in recent decades; this makes it one of the most promising polymers. The high viscosity of UHMWPE above the melting temperature ( $T_m$ ) restricts its processing with screw extrusion or injection molding. UHMWPE is very frequently processed via hot pressing or the sintering of cold-pressed billets. Such processing methods allow one to use powders as starting materials; this may be very useful in the case of UHMWPE-based composite production. Powder technology allows one to apply various solid-state methods to produce polymer-based composites, including a method of high-energy ball milling (HEBM).<sup>1–7</sup> This method implies the application of severe plastic deformation to the polymer matrix; this can give rise to different structural changes in the polymer. In this regard, it is important to understand the effects of such deformation on the polymer structure. The severe deformation of polymers can lead to different structural changes that are caused by the movement of molecular chains at the intermolecular level; this can strongly affect the properties of the polymers. These changes depend on the nature of the polymer and the deformation conditions. In most cases, deformation results in structural alterations, amorphization, and/or phase transitions.

It is known that milling can result in phase transformations and the amorphization of polymers. For instance, the milling of high-density polyethylene (HDPE) leads to the transformation of the orthorhombic phase into a monoclinic one.<sup>8,9</sup> Poly(vinylidene fluoride) transforms from the  $\alpha$  to the  $\beta$  phase under milling,<sup>10</sup> whereas the high-energy milling of poly(vinyl acetate),<sup>11</sup> polyamide 6,<sup>12</sup> and polypropylene<sup>13</sup> leads to the amorphization of the crystalline phase. The deformation of polymers can also be accompanied by a decrease in the molecular weight, changes in the morphology and size of the crystalline particles, and the oxidation and formation of crosslinked structures.<sup>8–10,13</sup> In this study, the effects of HEBM on the UHMWPE structure and properties were examined.

### EXPERIMENTAL

Ticona GmbH GUR 4120 UHMWPE-grade, with a molecular weight of  $5 \times 10^6$  g/mol, was used in this investigation. Deformation processing was carried out in an MPF-1 high-energy planetary ball mill in 0.4-L steel vials. As the grinding media, we used steel balls with diameters from 5 to 9 mm and a total weight of 900 g (5 mm and 200 g, 7 mm and 200 g, and 9 mm and 500 g). The mass of the polymer loaded into the steel drum was 60 g. The carrier's rotation speed was constant and equal to 900 rev/min. The duration of mechanical treatment ranged from 5 min to 2 h.

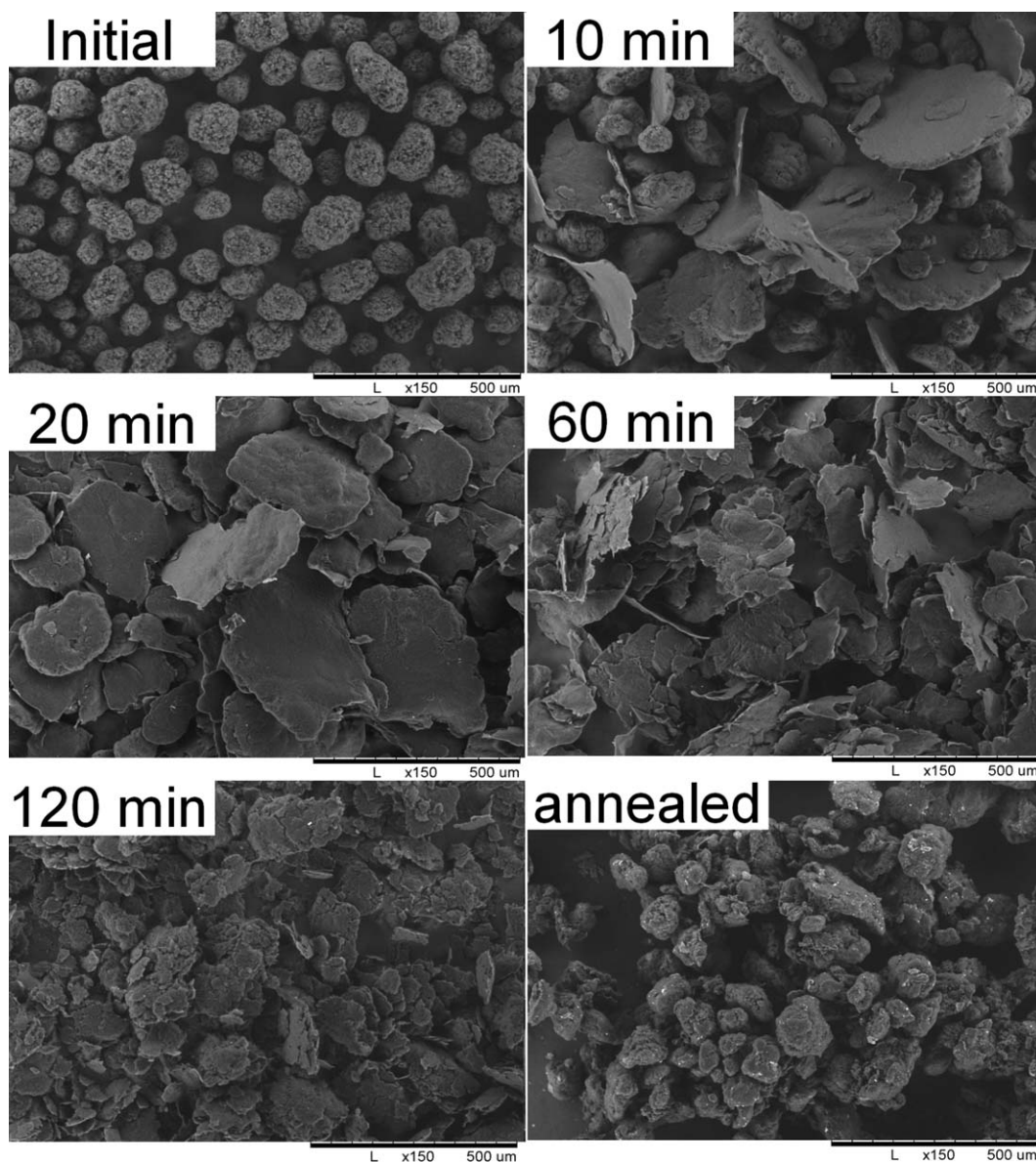


**Figure 1.** Evolution of the UHMWPE morphology during milling; the processing times are indicated on the micrographs. The figure also shows a micrograph of powder milled for 20 min and then annealed above  $T_m$ .

Micrographic investigations were carried out with a low-vacuum scanning electron microscope (Hitachi TM-1000). The phase composition and crystalline structure of the powders were studied by X-ray analysis on a Rigaku Ultima IV diffractometer with monochromatized Cu K $\alpha$  radiation. The parameters of the fine structure were determined by analysis of the broadening of the diffraction lines by Ritveld's method.<sup>14</sup> Thermal analysis of the treated powder was carried out with differential scanning calorimetry (DSC) on a Netzsch DSC 204 F1 calorimeter in an argon atmosphere. DSC experiments were carried out under the following conditions: heating from 35 to 180°C, 5 min of exposure, cooling to 35°C, 5 min of exposure, and the second heating up to 180°C, and a heating and cooling rate of 10°C/min. The key parameters for DSC processing were as follows: the onset of the melting peak ( $T_m^{\text{onset}}$ ), the melting

temperature peak ( $T_m^{\text{max}}$ ), the melting heat ( $\Delta H_m$ ), the onset of the crystallization peak ( $T_c^{\text{onset}}$ ), the crystallization temperature peak ( $T_c^{\text{max}}$ ), and the crystallization heat ( $\Delta H_c$ ). The consolidation of the powders was carried out by hot pressing under a pressure of 60 MPa; the consolidation temperatures were varied from 137 to 210°C. The mechanical properties were investigated with an Instron 150LX tensile machine with a loading rate of 10 mm/min.

## RESULTS AND DISCUSSION

The morphological evolution of the UHMWPE powder during milling is shown in Figure 1. The initial UHMWPE particles were spherical, with an average size of 120  $\mu\text{m}$ . During the application of severe deformation, the polymer powder particles

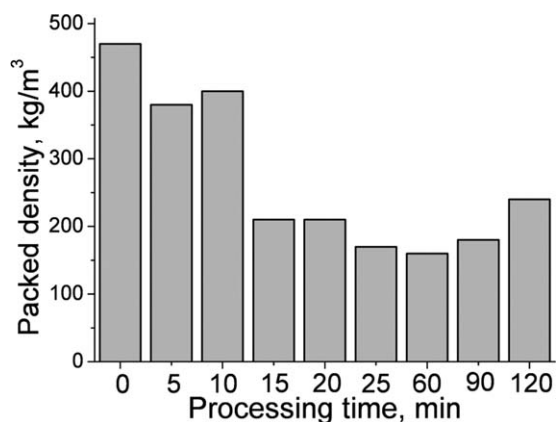


**Figure 2.** Packed density of UHMWPE as a function of the processing time.

gradually changed their morphology, and after 20 min of milling, all of the particles acquired a lamellar shape. The formed lamellas were less than 10  $\mu\text{m}$  in thick and about 270  $\mu\text{m}$  in diameter. After 60 min of milling, delamination began to appear on the lamellae. Milling for 90 min resulted in the separation of flattened powder particles into smaller ones, and, finally, powder milled for 120 min contained a number of small lamellar particles (<50  $\mu\text{m}$  in diameter). It is necessary to note that powder milled for 20 min, where initially spherical particles already took lamellar form but did not yet start to split into smaller ones, after annealing above  $T_m$  regained their initial spherical shape. This was evidence of the shape-memory effect in UHMWPE, which we studied recently.<sup>15</sup>

These data correlated well with those on the packed density of UHMWPE powder as a function of the processing time (see Figure 2). As the form of the particles under deformation changed from a close to a spherical to a flat shape, the average size of the particles increased, and the packed density decreased. With further increases in the processing time, the polymer particles were crushed, and the packed density again began to rise. A decrease in the aspect ratio by the comminution of flat particles to spherical ones resulted in an increase in the packed density.<sup>16</sup>

It should be mentioned that the deformation of UHMWPE particles inevitably led to an orientation of the molecules. Figure 3 shows the scheme of the UHMWPE microstructure evolution with ball milling. The polymer particles were strongly flattened and took a flake shape; this was accompanied by a triple

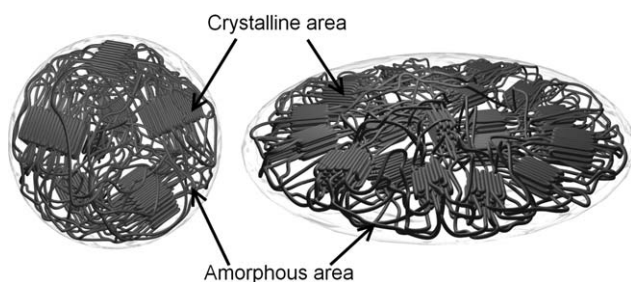


**Figure 3.** Scheme of the stress-induced structure orientation of UHMWPE: (left) the initial UHMWPE particle and (right) the particle after the impact blow.

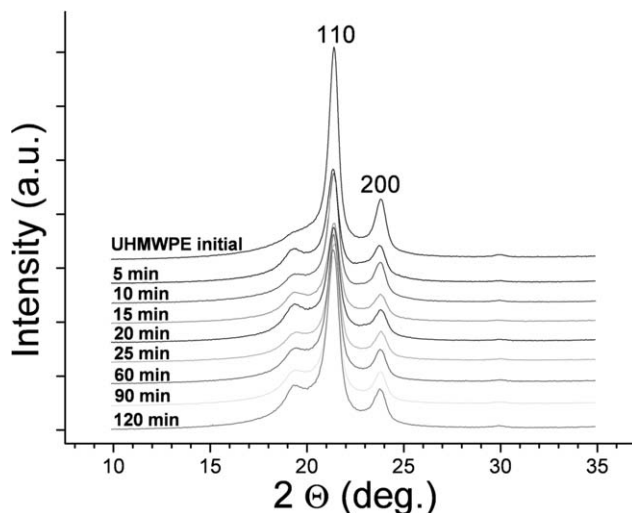


**Figure 4.** X-ray diffraction patterns of the initial and ball-milled UHMWPE powders.

increase in its plane size. Both the amorphous and crystalline phases took up orientation of the plane perpendicular to the applied impact. Structural orientation as the result of polymer particles flattening during ball milling has also been proposed for polyethylene (PE)<sup>17</sup> and poly(ethylene terephthalate).<sup>18,19</sup>

Changes in the structure of the treated polymer powders were studied with X-ray diffraction analysis. Figure 4 shows that whereas before the deformation the UHMWPE powder preferentially consisted of an amorphous phase (a halo with center at  $2\theta = 19.45^\circ$ ) and an orthorhombic crystalline phase [with two intensive peaks at  $2\theta = 21.5^\circ$  (110) and  $2\theta = 23.9^\circ$  – (200)], after deformation a new peak appeared at  $2\theta = 19.55^\circ$ . This peak corresponded to the monoclinic phase, which is usually formed in PEs as a result of deformation processes, including ball milling.<sup>8,9,17,20</sup> An increase in the milling time resulted in an increase in the related monoclinic phase peak intensity. Analysis of broadening of the diffraction lines showed that the crystallite size of the orthorhombic phase (D) decreased during milling (Figure 5), whereas the magnitude of microstrains remained constant and equal to 0.8%.

Figure 6 shows the DSC curves (first heating) for the initial and as-milled UHMWPE powders; the temperatures of the melting

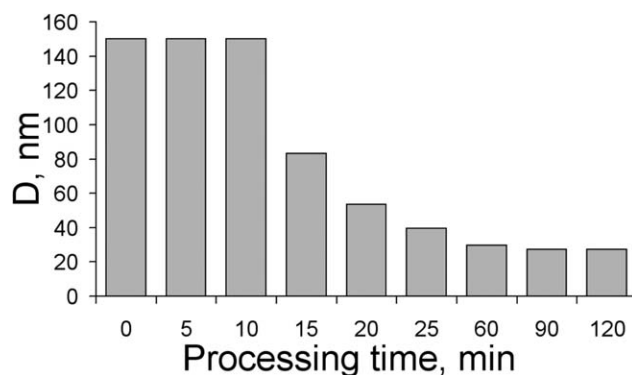


**Figure 5.** Crystallite size of orthorhombic phase (D) as a function of the processing time.

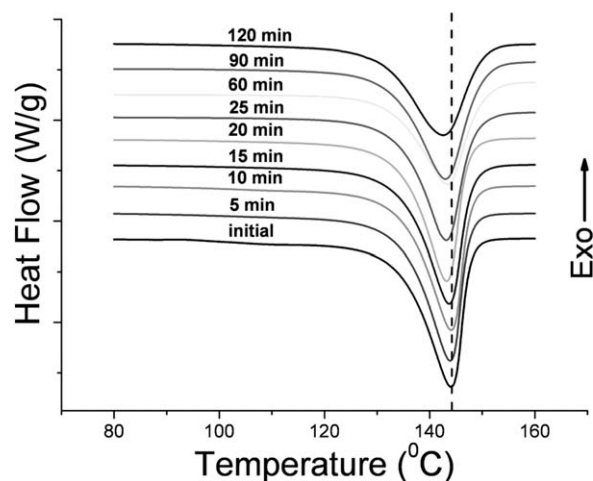


**Figure 6.** DSC curves (first heating cycle) of the initial and milled UHMWPE powders; the milling times are indicated near the curves.

peaks and the heat effect of melting are listed in Table I. In the first cycle of heating, with increasing milling time, both  $T_m^{\text{onset}}$  and  $T_m^{\text{max}}$  decreased. Compared with the initial UHMWPE powder, after 120 min of milling,  $T_m^{\text{onset}}$  decreased by 4°C, and  $T_m^{\text{max}}$  decreased by 1.6°C. Such a decrease in  $T_m$  could have been due to a decrease in the molecular weight brought about by the rupture of the polymer chains under the impact load in a ball mill. However, as shown in ref. 21, when the molecular weight of PE exceeded the value of  $10^5$ – $10^6$  g/mol, its magnitude did not affect  $T_m$ .

The  $T_m$  values of the polymers may have also depended on the thickness of lamellar crystallites (e.g., see ref. 22). A decrease in the lamellar size and an increase in the concentration of the defects in the crystalline structure resulted in a decrease in  $T_m$  according to Thomson–Gibbs:

$$T_m = T_m^0 (1 - 2\sigma_e / (\Delta H \times l)) \quad (1)$$

where  $T_m^0$  is the melting temperature of the lamellar crystals of infinite size,  $\sigma_e$  is the surface energy,  $\Delta H$  is the melting enthalpy, and  $l$  is the thickness of the lamellar crystal. The DSC analysis results allowed us to propose that the ball milling of UHMWPE resulted in a decrease in the lamellar thickness and/or an increase in the defect concentration in the crystalline structure. Comparing the DSC data with the results of X-ray diffraction (see Figure 5), we concluded that a decrease in  $T_m$  was associated with a decrease in the lamellar thickness. X-ray diffraction showed no changes in the microstrains; this was related to the defects in the crystalline structure as a result of milling. In ref. 17, similar results were observed for ball-milled HDPE.

As shown in Table I,  $\Delta H$  of UHMWPE decreased with increasing the milling time. The relative degree of crystallinity was calculated as the ratio of  $\Delta H_m$  of the experimental sample to  $\Delta H_m$  of the completely crystallized PE, which, according to ref. 23, is equal to 288 J/g. The calculations showed that the mechanical treatment of UHMWPE powder led to its partial amorphization. Thus, the degree of crystallinity of the initial powder was 64%, whereas after 120 min of mechanical treatment, it decreased to 51%.

The process of crystallization in polymers is a complex process that depends on the thermal and deformation history undergone by the material.<sup>24</sup> Cooling after the first heating showed no deviation in the calorimetric parameters during the crystallization of the milled samples from those in the initial state (see Table I, column 2). It showed that the initial and milled UHMWPE after melting possessed similar thermal properties, and those acquired by milling structural features disappeared after melting.

In the second cycle of heating,  $T_m$  increased slightly (on average by 1°C). The degree of crystallinity of UHMWPE after remelting also increased by 2–5% for the sample deformed for 25 min. These facts could have been explained by powder contamination with iron from the milling media; iron particles could have later acted as a nucleation agent of heterogeneous crystallization. Figure 7 shows the spectra of X-ray fluorescence analysis of the deformed UHMWPE powder. With increasing processing time, there was an increase in the intensity of the peaks responsible for the presence of iron. Apparently, after 25 min of milling, the process contamination of iron accumulated in the treated powder became sufficient to affect the crystallization process of the polymer.

Without the effect of iron contamination on the crystallization process of UHMWPE taken into account, all structural alterations of the polymer caused by deformation treatment were erased after remelting.

It is worth noting that in HDPE after HEBM,<sup>20</sup> the separation of the crystallization peak was observed (double crystallization; the DSC shooting conditions were the same as ours), the authors put forward the assumption of the high thermal stability of the monoclinic-phase nucleating agent and the possibility of the second formation of this phase after the melting down of the polymer in case it had been in the molten state only for a small time. However, in one of our earlier studies,<sup>25</sup> we carried out the annealing of the deformed UHMWPE, and this experiment showed the metastability of the monoclinic phase. The metastability of the monoclinic phase was also confirmed by other authors.<sup>9,26</sup> Such a divergence in the experimental results could be caused by the different conditions of the deformation process and the different molecular weights of the polymers used.

It ought to be noted that in ref. 17, the authors obtained the data on the opposite effect of preliminary deformation treatment on DSC curves. For HDPE, an increase in the duration of cryogenic mechanical milling (CMM) resulted in an increase in the  $\Delta H_m$  values obtained both from the first and second cycles of heating. The authors suggested that in the process of CMM, the molecular weight of the amorphous phase of HDPE selectively decreased. Reducing the molecular weight decreased the degree of entanglements so that defect-free polymer segments were allowed to attain easier crystallization.

A study of the effect of the pan-milling stress on the structure of HDPE<sup>8</sup> showed that the molecular weight decreased gradually with milling time. Moreover, at the higher initial molecular weight, easier degradation could be achieved under stress.

**Table I.** Results of the DSC Analysis

| UHMWPE  | First heating cycle       |                         |                    | Cooling cycle             |                         |                    | Second heating cycle      |                         |                    |
|---------|---------------------------|-------------------------|--------------------|---------------------------|-------------------------|--------------------|---------------------------|-------------------------|--------------------|
|         | $T_m^{\text{onset}}$ (°C) | $T_m^{\text{max}}$ (°C) | $\Delta H_m$ (J/g) | $T_c^{\text{onset}}$ (°C) | $T_c^{\text{max}}$ (°C) | $\Delta H_c$ (J/g) | $T_m^{\text{onset}}$ (°C) | $T_m^{\text{max}}$ (°C) | $\Delta H_m$ (J/g) |
| Initial | 134.4                     | 144.0                   | 184.8              | 122.7                     | 118.0                   | 129.0              | 125.7                     | 134.8                   | 140.5              |
| 5 min   | 134.4                     | 143.9                   | 178.1              | 122.7                     | 118.1                   | 121.1              | 125.8                     | 134.8                   | 136.7              |
| 10 min  | 134.4                     | 144.1                   | 178.5              | 122.5                     | 117.9                   | 117.9              | 125.8                     | 135.0                   | 135.5              |
| 15 min  | 134.2                     | 143.7                   | 173.0              | 122.7                     | 117.9                   | 129.8              | 125.7                     | 135.0                   | 142.1              |
| 20 min  | 134.0                     | 143.2                   | 170.0              | 122.8                     | 118.3                   | 127.2              | 125.6                     | 134.5                   | 139.2              |
| 25 min  | 134.0                     | 143.1                   | 165.4              | 122.7                     | 118.2                   | 131.5              | 125.5                     | 135.8                   | 138.0              |
| 60 min  | 133.7                     | 143.1                   | 165.6              | 121.8                     | 118.0                   | 132.5              | 125.9                     | 136.2                   | 148.0              |
| 90 min  | 132.0                     | 143.0                   | 177.1              | 122.2                     | 118.2                   | 140.2              | 125.7                     | 135.6                   | 158.2              |
| 120 min | 130.4                     | 142.6                   | 149.2              | 122.4                     | 117.3                   | 133.2              | 126.0                     | 136.1                   | 148.4              |

In Ref. 27, it was noted that the HEBM processing of medium-density PE had little effect on the crystalline temperature and  $T_m$  of the initial polymer and its nanocomposites. The investigation of HDPE<sup>20</sup> by size exclusion chromatography after treatment in HEBM indicated no changes in the molecular weight distribution.

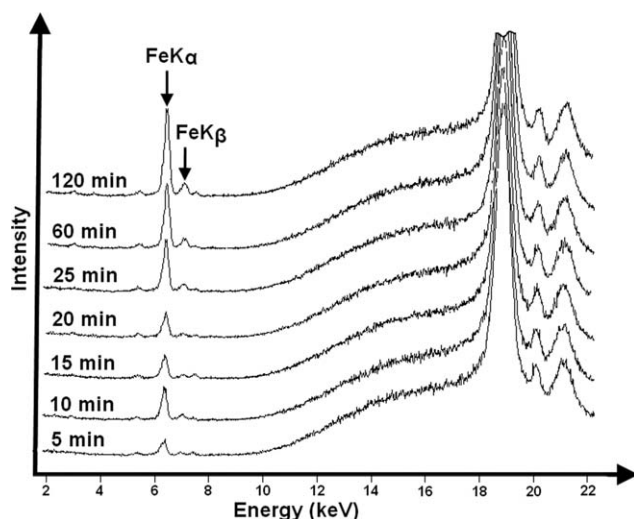
As shown, the treatment of PE in mills may have different effects on the molecular weight. This depends on the type of mill and the conditions of processing. PE has a relatively high chain mobility at ambient temperature. Under the action of impact stress, the mobile molecular chains are deformed without breaking. Therefore, HEBM processing was not accompanied by degradation of the polymer. During the processing of PE in CMM below the glass-transition temperature, the polymer molecular mobility was greatly reduced, and the impact stress led to a decrease in the molecular weight. However, UHMWPE could perform its functions without degradation, even below the glass-transition temperature. The CMM processing of UHMWPE requires further study. The pan-mill-type equipment can exert strong shear force on materials, even

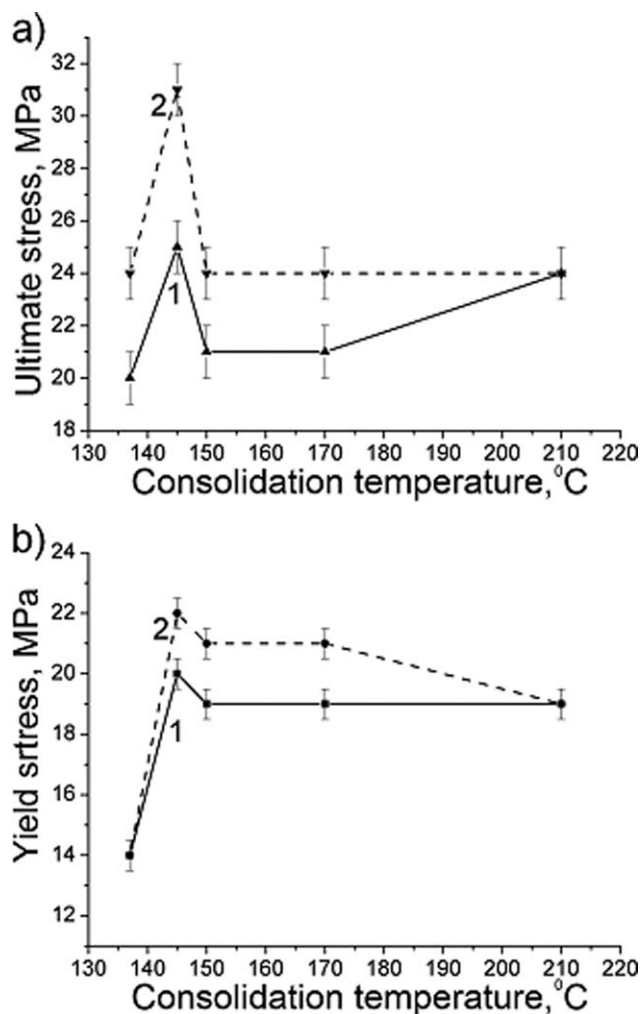
greater than planetary mills. Under pan-milling stress, PE chains experience strong stretching, which results in molecular rupture, even at room temperature.

Figure 8(a,b) presents the ultimate and yield tensile stress as function of the pressing temperature for the initial and pre-treated samples. The minimum strength value was observed after consolidation at 137°C; this was associated with the incomplete partial melting of the crystalline part of the polymer, which resulted in a relatively weak interaction between the powder particles at consolidation. The maximum strength characteristics for both the initial sample and preliminarily treated UHMWPE was observed at a consolidation temperature of 145°C. For the initial UHMWPE, such an increase in the strength was due to the better sintering between the powder particles and the partial conservation of the nascent crystallinity, which toughened the polymer.<sup>28</sup> The ultimate stress of the pre-treated UHMWPE increased by 6 MPa [Figure 8(a)], and its yield stress increased by 2 MPa [Figure 8(b)] compared to the initial polymer. With further increases in the formation temperature, the yield and ultimate tensile stress of the UHMWPE began to decrease, and at 210°C, they leveled out with the characteristics of the initial polymer.

Figure 9 shows the relative elongation of the samples as a function of the hot-pressing temperature. In the range of hot-pressing temperatures from 137 to 145°C, the elongation of the pretreated UHMWPE sample was significantly lower compared to that of the initial polymer. After an increase in the pressing temperature to 150°C and higher, the elongation values both for the initial and milled UHMWPE became nearly the same.

The observed peculiarities of changes in the mechanical properties with consolidation temperature for the initial and ball-milled UHMWPE could be explained by the retention of the oriented structure in the polymer powder up to a pressing temperature of 145°C and the restoration of the isotropic properties of the polymer powder at temperatures above 150°C. To confirm our assumption, we carried out an additional experiment. To decorate the structure of the polymer, we added nanosized tungsten powder into the initial and ball-milled UHMWPE powders. The distribution of nanotungsten over the surface of

**Figure 7.** Spectra of the X-ray fluorescence analysis of the deforming treatment of the UHMWPE powder.



**Figure 8.** (a) Ultimate and (b) yield tensile stress as a function of the consolidation temperature for the (1) initial sample and (2) sample preliminarily treated in a ball mill UHMWPE samples.

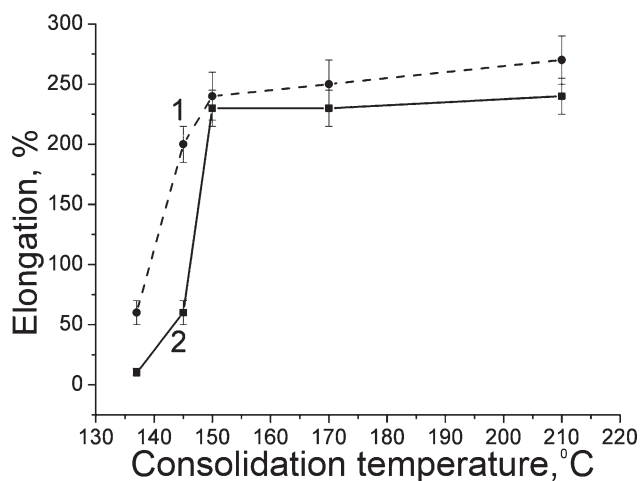


**Figure 9.** Percentage elongation of the UHMWPE samples: (1) initial sample and (2) sample preliminarily treated in a ball mill as a function of hot temperature.

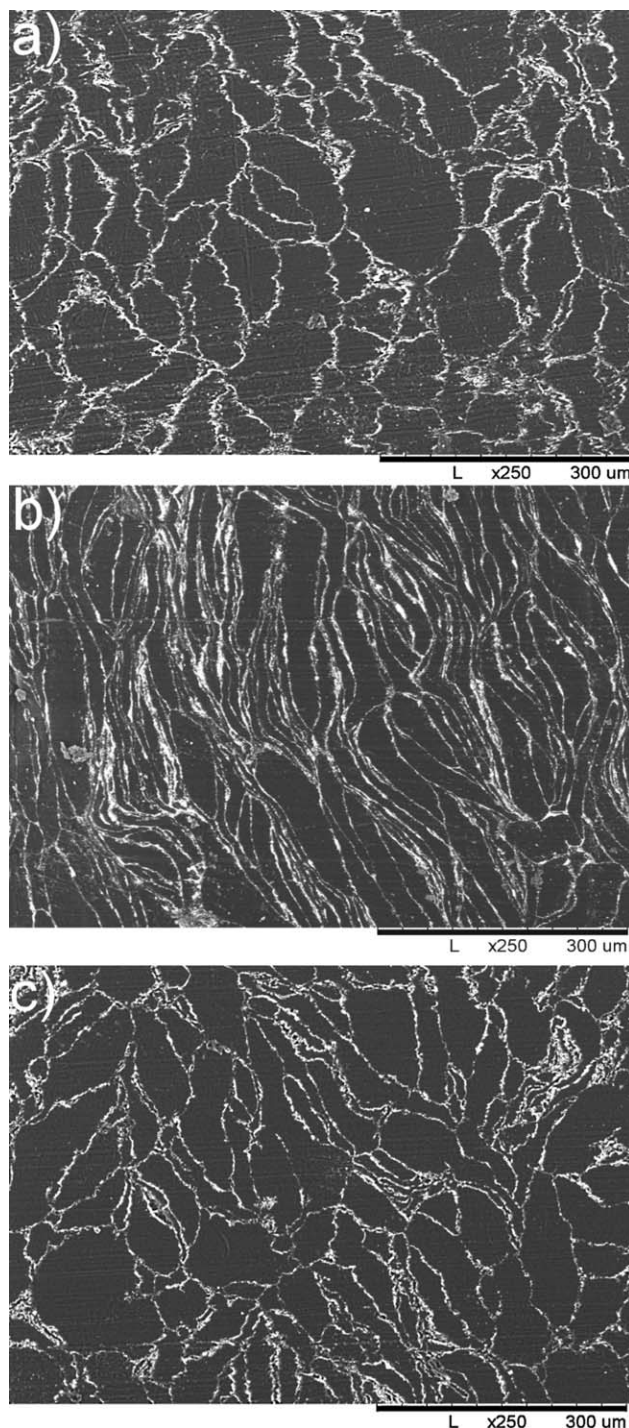


**Figure 10.** Decorated structure of (a) the initial UHMWPE, (b) pretreated UHMWPE after pressing at 145 °C, and (c) pretreated UHMWPE after pressing at 160 °C.

the UHMWPE powder was carried out in a planetary ball mill in decorated operation conditions so as not to affect the structure of the polymer. The mixture of UHMWPE with nano-tungsten was carried out in a planetary ball mill (Fritsch Pulverisette 5). The conditions of mixing were as follows: diameter of steel balls = 10 mm, total weight = 600 g, rotation speed = 150 rev/min, and duration of mixing = 60 min. The

obtained powders were pressed at temperatures of 145 and 160°C. Thin cross-sectional slices were prepared from the samples and were then studied with scanning electron microscopy. With simultaneous treatment in the mill of the polymer powder with the nanopowder, it uniformly covered the polymer particles and, after consequent thermal consolidation, this clearly indicated the borders of the polymer particles in the bulk state. The micrographs shown in Figure 10 clearly demonstrate the shape and arrangement of the UHMWPE powder particles in a monolithic sample after hot pressing. The particles of the initial UHMWPE powder [Figure 10(a)] were slightly flattened and elongated with exposure to pressure. The powder particles of the pretreated UHMWPE pressed at 145°C [Figure 10(b)] were characterized by the conservation of their shape acquired after the preliminary deformational treatment. The UHMWPE powder particles retained an oriented structure, which was responsible for the increased mechanical properties and reduced elongation. When the pretreated UHMWPE sample was pressed at temperatures over 145°C, [Figure 10(c)], the powder particles regained their initial shape, their orientation disappeared, and their mechanical properties and elongation returned to values equal to those of the initial UHMWPE. The recovery of the initial shape in the UHMWPE powders under temperature exposure is described in ref. 14.

## CONCLUSIONS

The deformation processing of the UHMWPE powder in a planetary ball mill led to a flattening of the initially spherical particles and the acquisition of an oriented structure. These processes were accompanied by amorphization, the acquisition of a defective crystal structure, and a new monoclinic phase formation. During annealing of the deformed powders, the polymer crystallized into a structure intrinsic for the initial UHMWPE; that is, that its deformation prehistory gets erased. The acquisition of an oriented structure by the monolithic UHMWPE samples pressed at 145°C resulted in an increase in their strength and a decrease in their percentage elongation. With increasing temperature, the properties of the pretreated UHMWPE tended to level out with those of the initial polymer.

## ACKNOWLEDGMENTS

This work was supported within the framework of a federal target program (Research and Development on the Priority Directions of the Development of Scientific and Technological Industry of Russia for 2007–2013) under state contract 16.513.11.3148.

## REFERENCES

1. Ishida, T.; Tamaru S. *J. Mater. Sci. Lett.* **1993**, *12*, 1851.
2. Zhu, Y. G.; Li, Z. Q.; Zhang, D.; Tanimoto T. *J. Polym. Sci. Part B: Polym. Phys.* **2006**, *44*, 1161.
3. Wang, G.; Chen, Y.; Wang Q. *J. Polym. Sci. Part B: Polym. Phys.* **2008**, *46*, 807.
4. Kaloshkin, S. D.; Tcherdyntsev, V. V.; Gorshenkov, M. V.; Gulbin, V. N.; Kuznetsov S. A. *J. Alloys Compd.* **2012**, *536S*, S522.
5. Kaloshkin, S. D.; Vandi, L. J.; Tcherdyntsev, V. V.; Shelekhov, E. V.; Danilov V. D. *J. Alloys Compd.* **2009**, *483*, 195.
6. Maksimkin, A. V.; Kaloshkin, S. D.; Tcherdyntsev, V. V.; Senatov, F. S.; Danilov V. D. *Inorg. Mater. Appl. Res.* **2012**, *3*, 288.
7. Maksimkin, A. V.; Kaloshkin, S. D.; Kalosnkina, M. S.; Gorshenkov, M. V.; Tcherdyntsev.; Ergin, K. S.; Shchetinin I. V. *J. Alloys Compd.* **2012**, *536S*, S538.
8. Huang, H. *J. Appl. Polym. Sci.* **2000**, *78*, 2016.
9. Stranz, M.; Koster, U.; Katzenberg F. *J. Metastable Nanocryst. Mater.* **2005**, *24–25*, 463.
10. Esterly, D.; Love B. *J. Polym. Sci. Part B: Polym. Phys.* **2004**, *42*, 91.
11. Molina-Boisseau, S.; Le Bolay N. *Powder Technol.* **2002**, *128*, 99.
12. Chen, Z.; Liu, C.; Wang Q. *Polym. Eng. Sci.* **2004**, *41*, 1187.
13. Stranz, M.; Koster U. *Colloid Polym. Sci.* **2004**, *282*, 381.
14. Maksimkin, A.; Kaloshkin, S.; Zadorozhnyy, M.; Tcherdyntsev V. *J. Alloys Compd.* [Online early access]. DOI: 10.1016/j.jallcom.2012.12.014. Published Online: Dec 13, 2012. <http://dx.doi.org/10.1016/j.jallcom.2012.12.014>. Accessed on 13 December 2012.
15. Shelekhov, E. V.; Sviridova T. A. *Metal Sci. Heat Treatment* **2000**, *42*, 309.
16. Wouthes, A.; Williams S. R.; Philipse A. P. *J. Phys. Condens. Matter.* **2007**, *19*, 1.
17. Barbosa, A. P. C.; Stranz, M.; Katzenberg, F.; Köster, U. *e-Polym.* **2009**, *096*, 1.
18. Bai, C.; Spontak, R. J.; Koch, C.; Saw, C. K.; Balike, C. M. *Polym.* **2000**, *41*, 7147.
19. Zhu, Y. G.; Li, Z. Q.; Zhang, D.; Tanimoto T. *J. Polym. Sci. Part B: Polym. Phys.* **2006**, *44*, 986.
20. Olmos, D.; Dominguez, C.; Castrillo, P. D.; Gonzalez-Benito, J. *Polymer* **2009**, *50*, 1732.
21. Hoffmann, J. D.; Frolen, L. J.; Ross, G. S.; Lauritzen, J. *J. Res. Natl. Bur. Stand. A* **1975**, *79*, 671.
22. Jiang, Q.; Yang, C. C.; Li, J. C. *Macromol. Theory Simul.* **2003**, *12*, 57.
23. Wunderlich, B.; Cormier, C. M. *J. Polym. Sci. Part A-2: Polym. Phys.* **1967**, *5*, 987.
24. Rao, I. J. *Int. J. Nonlinear Mech.* **2003**, *38*, 663.
25. Maksimkin, A. V.; Kaloshkin, S. D.; Tcherdyntsev, V. V.; Ergin K. S. *Deformation Fracture Mater.* **2010**, *12*, 10.
26. Castricum, H. L.; Yang, H.; Bakker, H.; Deursen J. H. V. *Mater. Sci. Forum.* **1997**, *211*, 235.
27. Tadayyon, G.; Zebarjad, S. M.; Sajjadi, S. A. *Int. Polym. Process* **2001**, *4*, 354.
28. Jauffres, D.; Lame, O.; Vigier, G.; Dore, F. *Polymer* **2007**, *48*, 6374.